

Near-relativistic electron acceleration by Landau trapping in time domain structures

F.S. Mozer, A. Artemyev, O.V. Agapitov, D. Mourenas, I. Vasko

▶ **To cite this version:**

F.S. Mozer, A. Artemyev, O.V. Agapitov, D. Mourenas, I. Vasko. Near-relativistic electron acceleration by Landau trapping in time domain structures. Geophysical Research Letters, 2016, 43 (2), pp.508-514 10.1002/2015GL067316 . insu-01372261

HAL Id: insu-01372261

https://insu.hal.science/insu-01372261

Submitted on 26 Oct 2016

HAL is a multi-disciplinary open access archive for the deposit and dissemination of scientific research documents, whether they are published or not. The documents may come from teaching and research institutions in France or abroad, or from public or private research centers.

L'archive ouverte pluridisciplinaire **HAL**, est destinée au dépôt et à la diffusion de documents scientifiques de niveau recherche, publiés ou non, émanant des établissements d'enseignement et de recherche français ou étrangers, des laboratoires publics ou privés.

AGU PUBLICATIONS

Geophysical Research Letters

RESEARCH LETTER
10.1002/2015GL067316

Key Points:
- Electrons are accelerated to near-relativistic energies by traveling parallel electric fields
- Such acceleration is due to Landau trapping of electrons in time domain structures
- This acceleration occurs in the Van Allen radiation belts and in other solar system plasmas

Supporting Information:
- Supporting Information S1

Correspondence to:
F. S. Mozer,
forrest.mozer@gmail.com

Citation:
Mozer, F. S., A. Artemyev, O. V. Agapitov, D. Mourenas, and I. Vasko (2016), Near-relativistic electron acceleration by Landau trapping in time domain structures, *Geophys. Res. Lett.*, *43*, 508–514, doi:10.1002/2015GL067316.

Received 7 DEC 2015
Accepted 8 JAN 2016
Accepted article online 9 JAN 2016
Published online 26 JAN 2016

©2016. American Geophysical Union. All Rights Reserved.

Near-relativistic electron acceleration by Landau trapping in time domain structures

F.S. Mozer[1], A. Artemyev[2,3], O.V. Agapitov[1,4], D. Mourenas[5], and I. Vasko[2]

[1]Space Sciences Laboratory, University of California, Berkeley, California, USA, [2]Space Research Institute, Russian Academy of Science, Moscow, Russia, [3]Institute of Geophysics and Planetary Physics, University of California, Los Angeles, California, USA, [4]Physics Department, Taras Shevchenko National University of Kyiv, Kiev, Ukraine, [5]LPC2E, CNRS-University of Orléans, Orléans, France

Abstract Data from the Van Allen Probes have provided the first extensive evidence of nonlinear (as opposed to quasi-linear) wave-particle interactions in space with the associated rapid (less than a bounce period) electron acceleration to hundreds of keV by Landau resonance in the parallel electric field of time domain structures (TDSs) traveling at high speeds (~20,000 km/s). This observational evidence is supported by simulations and discussion of the source and spatial extent of the fast TDS. This result indicates the possibility that the electrostatic fields in TDS may generate the electron seed population for cyclotron resonance interaction with chorus waves to make higher-energy electrons.

1. Introduction

Extensive observations by the Van Allen Probes of structures that carry large parallel electric fields at velocities greater than several thousand km/s, such as oblique chorus waves or time domain structures (electrostatic and electromagnetic phase space holes, double layers, solitary waves, nonlinear whistlers, etc.) [*Mozer et al.*, 2013, 2014, 2015], suggest the possibility of electron acceleration by Landau resonance trapping of particles in the effective potential well formed by the parallel electric fields of such structures and the action of the mirror force on particles in an inhomogeneous geomagnetic field. Experimental confirmation of Landau resonance electron acceleration to hundreds of keV by oblique chorus waves has been demonstrated [*Agapitov et al.*, 2015a].

Time domain structures (TDSs) are observed throughout the solar system [*Mozer et al.*, 2015, and references therein] and in huge quantities in the outer Van Allen radiation belts [*Mozer et al.*, 2013]. They are millisecond duration structures that propagate along the magnetic field, that may be electrostatic or electromagnetic, and that contain significant parallel electric fields. They have also been called electron holes, double layers, phase space holes, solitary waves, etc. An ideal electron hole is a positive potential structure whose electric field has the wrong sign to accelerate an electron that it overtakes. Thus, an electron-accelerating TDS must have a negative potential, at least in part. Because the potential structures of TDS are observed to vary in space over a distance of kilometers, or time over an interval of milliseconds, characterization of such structures as anything other than TDS is difficult and the criterion of importance in such considerations will be the existence and size of the negative potential in the structures. Following their observation by the Van Allen Probes, theories, simulations, and observations of the acceleration process have shown that a thermal electron can be accelerated to ~10 keV by interaction with electron-acoustic TDS whose parallel velocities of a few thousand km/s (the order of the electron thermal speed) make them capable of trapping thermal electrons [*Artemyev et al.*, 2014; *Vasko et al.*, 2015a]. However, as illustrated in Figure 1, TDS may also accelerate electrons to more than a hundred keV. During the event in this figure, at $L = 5.5$, magnetic local time (MLT) around 22:20, magnetic latitude = 11.6°, the 31 keV to 108 keV field-aligned electron flux exceeded that at 90° by factors of about 2 for up to 2 min. Field-aligned electrons at similar energies were earlier observed on GEOS 2 [*Kremser et al.*, 1988]. The highest energy of accelerated electrons among the 10 events that have been studied is about 300 keV.

2. Observations

The environment and particle measurements during this event show that the 100 keV acceleration was produced by TDS and not by chorus waves, injection, azimuthal drift, or adiabatic effects. Because the temporal modulation of the 90° electron fluxes in Figure 1 and the increases of the 25° to 90° flux ratio occurred

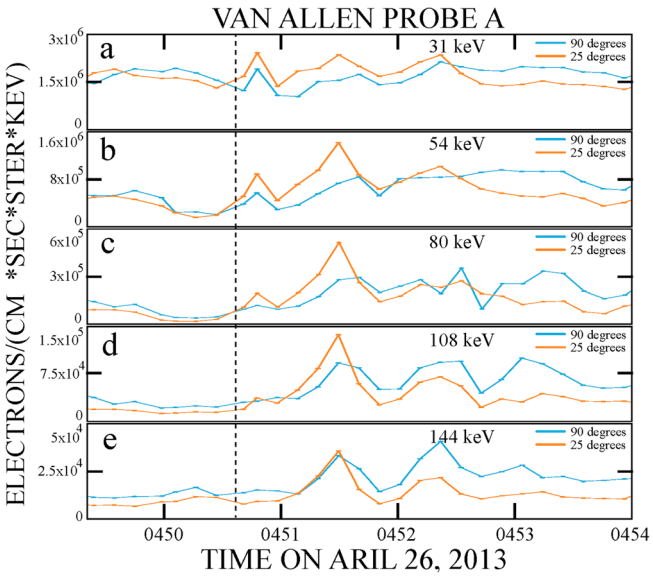


Figure 1. Illustrating that electrons from 31 keV to 144 keV had field-aligned pitch angle distributions because the 25° flux at each energy exceeded the 90° flux.

simultaneously at all energies from 31 keV to 143 keV during the period of interest, such increases of field-aligned electron fluxes must have been produced locally and not by the different azimuthal drift velocities of electrons of different pitch angles (or energies) coming from an injection zone at a different MLT [*Schulz and Lanzerotti*, 1974]. The magnetic field in Figure 2a was essentially constant, which implies that there were no adiabatic effects during the time of interest, as further confirmed by the absence of field alignment at energies larger than 140 keV (see Figure 1). Figure 2d presents the omnidirectional electron number flux above 20 keV. It shows an injection shortly after 04:45 universal time (UT), about 4 min before the field-aligned electron observations. Although this injection was not correlated in time with the acceleration because the pitch angle distribution of the injected electrons peaked at 90°, the injection may have provided the free energy that resulted in TDS generation [*Malaspina et al.*, 2015]. Figure 2b gives the electric field spectrum as a function of time. The red line in this panel is the electron gyrofrequency, and the white lines below it are at 0.5, 0.1, and 0.025 times this frequency, respectively. There were no chorus or other waves in this higher-frequency range during the time of interest, and the level of low-frequency electromagnetic noise (e.g., Alfven or electromagnetic ion cyclotron waves) was very low. However, there were intense electrostatic signals below about 100 Hz, called broadband electrostatic noise, that are the signature of TDS [*Matsumoto et al.*, 1994]. An example of the TDS seen throughout this event is given in Figure 3 which presents a 40 ms example of the TDS observed near the time of the 100 keV accelerated electrons. It gives the three components of the electric field in Figures 3a–3c and the magnetic field in Figures 3d–3f in magnetic-field-aligned coordinates, with the parallel electric and magnetic fields in Figures 3c and 3f, respectively. These data consist of a mixture of electron-acoustic solitons [*Mozer et al.*, 2013; *Artemyev et al.*, 2014] and electromagnetic (because the spiky structures were also observed in the magnetic field) three-dimensional (because the spiky structures were seen in all three components of the electric field) bipolar electron holes [*Mozer et al.*, 2015; *Vasko et al.*, 2015b]. TDS of both types have parallel electric field amplitudes as large as 40 mV/m. Such three-dimensional electromagnetic TDS have been observed in every one of the approximately 10 different events that have been studied in detail.

Figure 2c presents the pitch angle ratio of electrons measured by the HOPE (oxygen, proton, and electron) instrument on the Van Allen Probes. The pitch angle ratio is defined as the ratio of the average flux at the two largest and smallest pitch angles divided by the average of the fluxes at the three pitch angles nearest 90°. A value greater than one indicates that the pitch angle distribution at that energy is field aligned. Because the pitch angle ratio was less than one at the time of injection, the pitch angle distribution of the injected electrons was peaked at 90°. It became field aligned during the time of interest due to acceleration of near-thermal electrons by electron-acoustic TDS, as has been described in the literature [*Artemyev et al.*, 2014; *Vasko et al.*, 2015a].

For electrons to be trapped and accelerated to hundreds of keV by TDS, the TDS velocity must be much greater than the ~3000 km/s that accelerates thermal electrons to ~10 keV, in order that the TDS be in Landau resonance with electrons initially having energies of several keV. To estimate the velocity of one of these TDS, the time required for the structure to pass along the magnetic field line from the electric field detector's sphere 1 to sphere 2 has been estimated in Figure 4 by forming the functions $\Delta V_1 = [V_1 - (V_3 + V_4)/2]$ and $\Delta V_2 = [V_2 - (V_3 + V_4)/2]$ (at the time of this data, spheres 1 and 2 were oriented along the

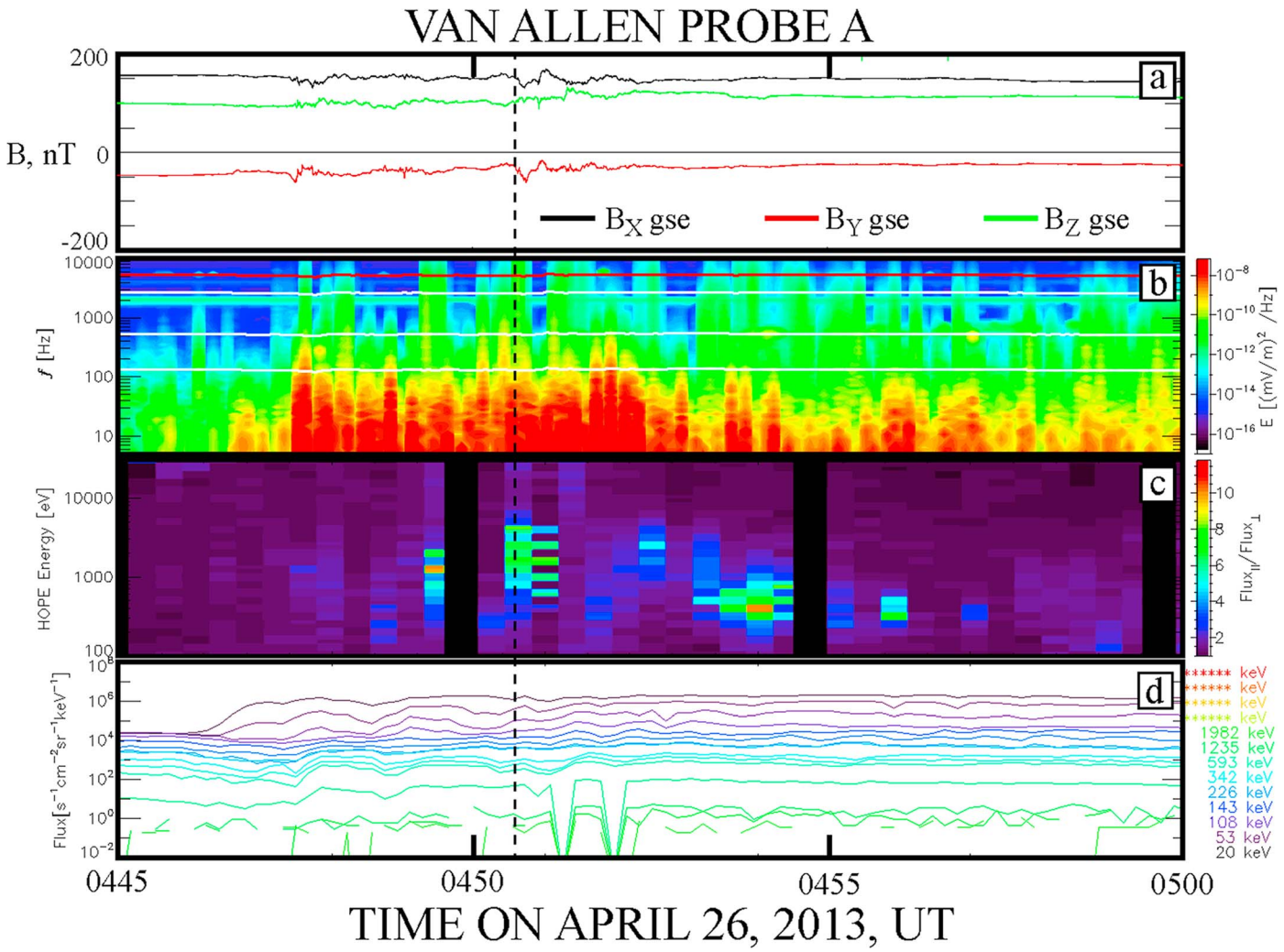


Figure 2. The environment at the time of the field-aligned 100 keV electron observations, showing that there were no adiabatic effects because the (a) magnetic field was essentially constant, there were (b) no whistlers but there was a large flux of TDS that produced the low-frequency broadband electrostatic noise, there were (c) no field-aligned electrons at the (d) 0446 plasma injection, and the plasma flux was approximately constant for 5 min before the 0452 observation of field-aligned electrons.

magnetic field line, while the line between spheres 3 and 4 was perpendicular to B). The motivation for these definitions follows from the fact that $V_n = v_n - v_{sc}$ where n is any of spheres 1 through 6, v_n is the potential of sphere n and v_{sc} is the potential of the spacecraft. (V_n quantities are potential differences, while v_n quantities are potentials. The individual potentials, v_n, cannot be measured because only potential differences are measureable.) The spheres are near their local plasma potentials because they are current biased, so v_n is also the potential of the plasma near sphere n, while the spacecraft is at a positive potential with respect to its local plasma that depends on the plasma density and other parameters. Thus, V_n depends on both the local plasma potential at sphere n and on plasma parameters associated with v_{sc}. It is desired to compare quantities associated with spheres 1 and 2 that depend only on their local plasma potentials. Because ΔV_1 is also equal to $[v_1 - (v_3 + v_4)/2]$, ΔV_1 measures the local plasma potential at sphere 1 relative to the local plasma potential at the location of the spacecraft, so that a comparison of ΔV_1 and ΔV_2 produces an estimate of the time required for the TDS to pass from sphere 1 to sphere 2, free of possible perturbations in the estimate associated with variations of the plasma properties.

Figure 4 presents a 250 μs duration plot of ΔV_1 and $-\Delta V_2$, during which time the TDS of interest crossed the spacecraft at the time given by the vertical dashed lines in Figures 1 and 2. The data in this figure were obtained at a rate of 16,384 samples per second, and there are five points in each panel because the TDS

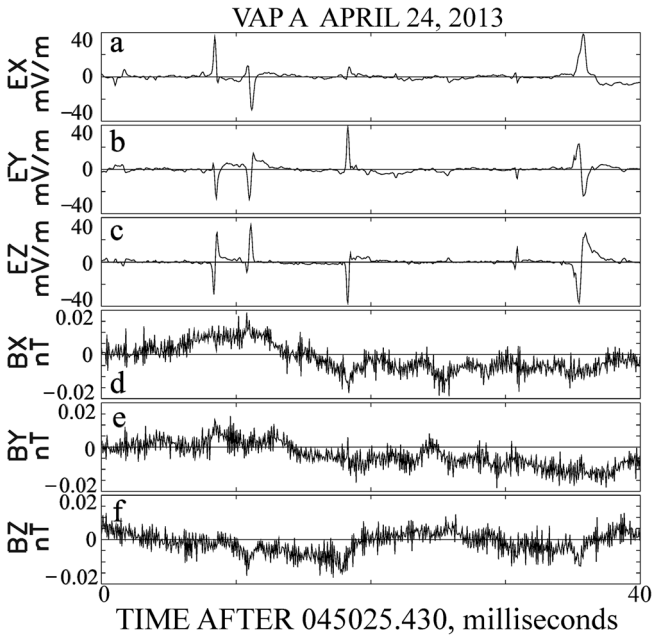


Figure 3. A 40 ms example of three components of the (a–c) electric field and the (d–f) magnetic field in magnetic-field-aligned coordinates, with the parallel electric and magnetic fields in Figures 3c and 3f, respectively. Because the spiky signatures of TDS are also seen in some of the magnetic field components, they are an example of electromagnetic TDS.

crossed the spacecraft in about 250 μs. Although the accuracy of the interferometry method is low because the TDS structure was greatly undersampled, a rough estimate of the time delay required for the TDS to pass from sphere 1 to sphere 2 can be provided by shifting their respective signals in time. The three panels correspond to delaying the second signal relative to the first by −2.5, 2.5, and 7.5 μs, respectively. (A correction for the fact that the V_1 measurement was digitized 3.85 μs before the V_2 measurement has been made when processing the data.) For time offsets of +2.5 and −7.5 μs, the $-\Delta V_2$ signal clearly lags or leads the ΔV_1 signal. Thus, a rough estimate of the time delay for the TDS signal to cross the 50 m separation from sphere 1 to the spacecraft is −2.5 μs, implying that the TDS was traveling at 20,000 km/s. A rough estimate of the uncertainty in this velocity is ±10,000 km/s, so the TDS was traveling sufficiently fast to trap more energetic electrons. The sign of this offset shows that the TDS was traveling away from the equator, which is required for significant electron acceleration, as discussed below.

It is useful to consider the 15 eV to 250 keV pitch angle distributions preceding and during the >100 keV acceleration event, as given in Figure 5 in which the wide green, yellow-green, red, purple, and blue lines are at energies of 1, 3, 10, 50, and 100 keV, respectively. In Figure 5a, 1 min before the acceleration, the 10 to 100 keV pitch angle distributions were peaked at 90° while, in Figure 5b, during the acceleration event, they were peaked at small pitch angles. Because the ratio of the measured fluxes at 10 keV and 108 keV was about 1000, the acceleration of about one 10 keV electron out of 1000 such electrons suffices to explain the observations. Another interesting feature is the plateau in the spectra in the few keV range, as evidenced by the bunching of the green curves in the two panels. In the presence of such a plateau in the background population, the observed fast TDS, which are presumably electron-acoustic solitons, should experience only weak Landau damping by the hot (keV) electron population, even though the latter density is much smaller than the cold (3–50 eV) plasma density [*Mace et al.*, 1999]. Finally, it is noted that the pitch angle distributions in the keV range were field aligned before and during the acceleration as a result of thermal electron acceleration by the slower TDS that appeared after about 0448 UT in Figure 2b.

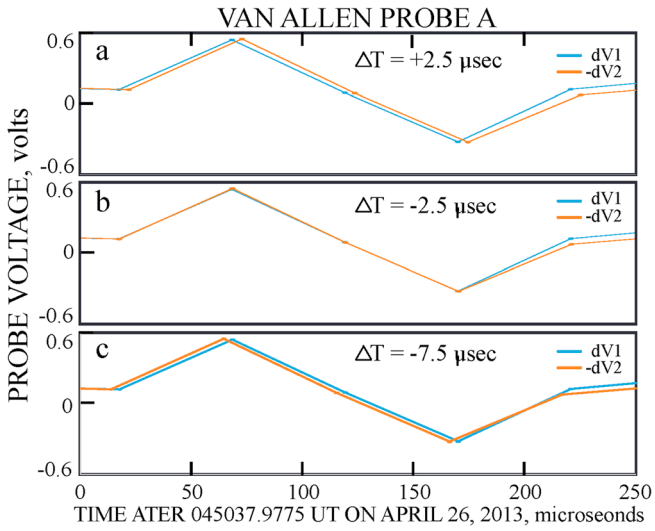


Figure 4. Comparison of signals on spheres 1 and 2 to estimate the time required for the TDS of interest to pass from sphere 1 to sphere 2. Because the two signals overlap for a time difference of −2.5 μs, the speed of the TDS to travel 50 m is estimated to be 20,000 km/s.

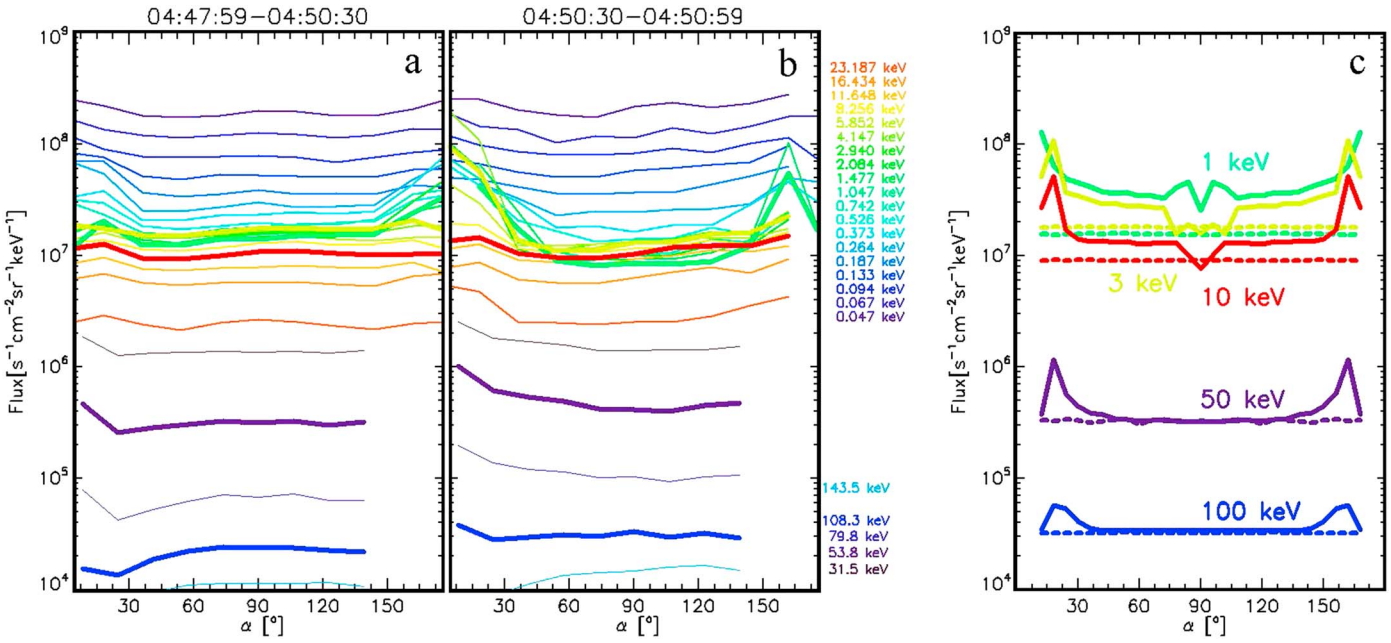


Figure 5. Pitch angle distributions of electrons from 15 eV to 150 keV, (a) one minute before the near-relativistic acceleration and (b) during the acceleration. Note that the flux of electrons at small pitch angles exceeds that at 90° for energies greater than 100 keV in Figure 5b. (c) Simulation results depicting electron acceleration by TDS are given. Note the similarity between the simulation and measured fluxes and pitch angles.

3. Discussion

Landau resonance trapping occurs when electrons that are moving away from the equator are overtaken by TDS whose parallel electric fields cause the electrons to be accelerated. If the electron parallel velocity is much smaller than the TDS velocity, the acceleration is short lived as the TDS passes by. If the electron parallel velocity is comparable to that of the parallel electric field, the electron may be trapped and accelerated to a higher velocity than that of the TDS and it will move away from the TDS. However, as the electron leaves the equator, it moves into a region of increasing magnetic field that causes its parallel velocity to be converted to perpendicular velocity. The electron's parallel velocity may then decrease such that it is overtaken by the parallel electric field structure and be further accelerated in a process that may be repeated many times. Thus, the electron can move at the roughly constant TDS parallel velocity while its perpendicular energy grows until the electron finally escapes from resonance. This process lowers the electron mirror point while it increases the electron energy, in such a way that the electron may either precipitate or return to the vicinity of the equator with a more field-aligned pitch angle distribution than it had when it left the equator. This acceleration occurs in a time less than the electron bounce period.

Suppose electrons start with energy E_o and pitch angle α_o at the equator where the magnetic field is B_o. Assuming that the first adiabatic invariant is conserved [*Shklyar and Matsumoto*, 2009] and that after acceleration the electron local pitch angle is close to 90°, the final E_m and B_m must be related roughly to initial values by $E_o \sin^2\alpha_o/B_o = E_m/B_m$, so that $E_m/E_o = (B_m/B_o)\sin^2\alpha_o$. The largest acceleration occurs for near-90° equatorial electrons that are trapped to the highest latitude that the TDS can travel before the electrons ultimately move out of resonance. Assuming that these fast TDS survive up to 40–45° magnetic latitudes (see discussion below), the corresponding upper bound on the B_m/B_o ratio is ~10. To accelerate a significant population of particles to 100 keV, TDS should then trap ~10 keV electrons around the equatorial plane. Considering the observed fast TDS propagating at about 20,000 km/s, the accelerated electrons should have initial resonant pitch angles $\alpha_o \sim 65°–75°$.

To model this acceleration process, the simulations presented in *Artemyev et al.* [2014] have been repeated, but with new parameters corresponding to the fast TDS discussed above. For the sake of simplicity, we focused here on the fast, negative potential, bipolar TDS seen in Figure 3 (while other types of observed TDS may have comparable effects, examining in detail the effects of all the different TDS would require a

separate study). The relative probabilities of electron interaction with different TDS are estimated from spacecraft measurements of distributions of TDS amplitudes and velocities. Namely, we use 20 different types of TDSs (five amplitudes 10, 20, 30, 40, and 50 mV/m and four values of the velocity 5000, 10000, 15000, and 20000 km/s) with the following distribution of amplitudes: 70% of TDSs have amplitude 10 mV/m, 19% of TDSs have amplitude 20 mV/m, 7% of TDSs have amplitude 30 mV/m, 3% of TDSs have amplitude 40 mV/m, and 1% of TDSs have amplitude 50 mV/m. Within each group of TDSs, the distribution over TDS velocity is as follows: 70% of TDSs have velocity 5000 km/s, 20% of TDSs have velocity 10000 km/s, 9% of TDSs have velocity 15,000 km/s, and 1% of TDSs have velocity 20,000 km/s. For example, there are ~49% of TDSs with 10 mV/m amplitude and velocity 5000 km/s, and only 0.01% of TDSs with 50 mV/m amplitude and 20000 km/s velocity.

An ensemble of 10^8 test particles was run with isotropic initial pitch angle distributions and energy spectra taken from spacecraft observations just before the acceleration process. As the interest is mainly associated with the nonlinear (trapping) interaction of electrons with TDS, the electron scattering by many TDS, described in *Vasko et al.* [2015a], has not been considered and, instead, the multiple interactions of an electron with a single TDS generated within 5° of the equatorial plane have been simulated, taking into account the mirror force of the geomagnetic field. It was assumed that the TDS decayed around 40–45° magnetic latitude (see discussion below). Considering a series of TDS with different parameters, one obtains different electron distributions after resonant interaction and, assuming that these distributions are independent of each other, the final, combined distribution of electrons interacting with a mixture of different TDS is obtained (this approach is essentially similar to the Green function approach proposed for nonlinear wave-particle interactions [*Artemyev et al.*, 2014; *Omura et al.*, 2015]). The relative probabilities of electron interaction with different TDS are estimated from spacecraft measurements of distributions of TDS amplitudes and velocities. Results for the final fluxes of accelerated electrons are shown in Figure 5c where the dashed lines represent the initial (uniform) pitch angle distributions and the solid lines represent the distributions of accelerated electrons. The comparison of initial and final fluxes demonstrates a clear increase of parallel fluxes for energies up to 100 keV, and the comparison of the simulation in Figure 5c with the observations in Figure 5b is good. (Note that in these simulations, some electrons were accelerated to 200 keV. This number would be increased greatly in the simulation by selecting faster TDS and larger fluxes of ~20 keV electrons.)

A crucial question remains to be addressed: How far from the equator can TDS actually propagate with trapped electrons, i.e., how large can B_m/B_o be? The observed TDSs represent electron-acoustic solitons existing in a plasma with cold and hot electron populations [*Fried and Gould*, 1961; *Watanabe and Taniuti*, 1977] and are quite analogous to ion-sound solitons in plasmas with hot electrons and colder ions [*Sagdeev*, 1966]. A full understanding of the influence of various dissipative mechanisms on TDS evolution and propagation would require a separate detailed study. Nevertheless, two points can already be mentioned here: (i) the flattened slope of the background parallel electron distribution observed in the vicinity of the velocity of fast TDS just before their appearance (see Figure 5) should mitigate Landau damping to some extent and (ii) observations of similar fast TDS up to the maximum latitude (~22°) reached by the Van Allen Probes, as well as on board the Polar satellite at $L \sim 5–7$ up to 45°–60° latitudes, suggest that the above-discussed model of TDS living to 40° of magnetic latitude seems quite reasonable.

Over a typical acceleration timescale of ~1 s (roughly corresponding to the time needed for the TDS to travel from +5 to +40° latitude at $L = 5–6$) electrons of less than 100 keV will experience an azimuthal drift around the Earth of less than 20 km. Thus, a relative homogeneity of the TDS and plasma medium over this scale is required for the proposed mechanism to work with its full efficiency. Moreover, this scale can be significantly reduced if one takes into account the 3-D configuration of TDS having a corresponding transverse electric field which induces a cross-field drift compensating drift due to magnetic field inhomogeneity.

One known mechanism for generation of the required fast TDS is through the nonlinear evolution of oblique chorus waves by wave-particle interactions [*Kellogg et al.*, 2011]. That such a process generates fast TDS is illustrated by the data given in the supporting information of this paper. Another possible method for generating fast TDS is through the same electron-acoustic interaction that produces slower TDS from a thermal population of a few tens of eV electrons, except that it now results from the population of 1–5 keV electrons.

In closing, it is noted that the processes that produce near-relativistic electrons in the Earth's outer radiation belt are general and not confined to that particular environment. Thus, one should expect that TDSs

accelerate electrons to high energies during magnetic field reconnection and on the Sun, other planets, and through the entire universe. In particular, a similar process may operate in the auroral region because the electrostatic turbulence observed in this region can be explained by the presence of electron-acoustic solitons [*Dubouloz et al.*, 1993].

Acknowledgments
The authors thank V. Krasnoselskikh and D. Malaspina for helpful discussions. The data used in this paper are available at the Van Allen Probe website, http://rbspgway.jhuapl.edu/. The authors thank the scientists and engineers associated with the EFW, EMFISIS, magEIS, and HOPE instruments for providing the high-quality data reported in this paper. The work by O.A. and F.M. was performed under JHU/APL contract 922613 (RBSP-EFW). A.V.A. is grateful to the Dmitry Zimin Dynasty Foundation for support. The work of I.Y.V. was supported by the Presidental grant MK-7757.2016.2.

References

Agapitov, O. V., A. V. Artemyev, D. Mourenas, F. S. Mozer, and V. Krasnoselskikh (2015a), Nonlinear local parallel acceleration of electrons through Landau trapping by oblique whistler-mode waves in the outer radiation belt, *Geophys. Res. Lett.*, *42*, 10,140–10,149, doi:10.1002/2015GL066887.

Artemyev, A. V., O. V. Agapitov, F. S. Mozer, and V. Krasnoselskikh (2014), Thermal electron acceleration by localized bursts of electric field in the radiation belts, *Geophys. Res. Lett*, *41*, 5734–5739, doi:10.1002/2014GL061248.

Dubouloz, N., R. A. Treumann, R. Pottelette, and M. Malingre (1993), Turbulence generated by a gas of electron-acoustic solitons, *J. Geophys. Res.*, *98*, 1741–17,422, doi:10.1029/93JA01611.

Fried, B. D., and R. W. Gould (1961), Longitudinal ion oscillations in a hot plasma, *Phys. Fluids*, *4*(1), 139–147, doi:10.1063/1.1706174.

Kellogg, P. J., C. A. Cattell, K. Goetz, S. J. Monson, and L. B. Wilson III (2011), Large amplitude whistlers in the magnetosphere observed with wind-waves, *J. Geophys. Res.*, *116*, A09224, doi:10.1029/2010JA015919.

Kremser, G., A. Korth, S. L. Ullaland, S. Perraut, A. Roux, A. Pedersen, R. Schmidt, and P. Tanskanen (1988), Field-aligned beams of energetic electrons (16 keV $< E <$ 80 keV) observed at geosynchronous orbit at substorm onsets, *J. Geophys. Res.*, *93*(A12), 14,453–14,464, doi:10.1029/JA093iA12p14453.

Mace, R. L., G. Amery, and M. A. Hellberg (1999), The electron-acoustic mode in a plasma with hot suprathermal and cool Maxwellian electrons, *Phys. Plasmas*, *6*, 44, doi:10.1063/1.873256.

Malaspina, D. M., J. R. Wygant, R. E. Ergun, G. D. Reeves, R. M. Skoug, and B. A. Larsen (2015), Electric field structures and waves at plasma boundaries in the inner magnetosphere, *J. Geophys. Res. Space Physics*, *120*, 4246–4263, doi:10.1002/2015JA021137.

Matsumoto, H., H. Kojima, T. Miyatake, Y. Omura, M. Okada, I. Nagano, and M. Tsutsui (1994), Electrotastic Solitary Waves (ESW) in the magnetotail: BEN wave forms observed by GEOTAIL, *Geophys. Res. Lett.*, *21*, 2915–2918, doi:10.1029/94GL01284.

Mozer, F. S., S. D. Bale, J. W. Bonnell, C. C. Chaston, I. Roth, and J. Wygant (2013), Megavolt parallel potentials arising from double layer streams in the Earth's outer radiation belts, *Phys. Rev. Lett.*, *111*, 235002.

Mozer, F. S., O. V. Agapitov, V. Krasnoselskikh, S. Lejosne, G. D. Reeves, and I. Roth (2014), Direct observation of radiation-belt electron acceleration from electron-volt energies to megavolts by nonlinear whistlers, *Phys. Rev. Lett.*, *113*, 035001.

Mozer, F. S., O. V. Agapitov, A. Artemyev, J. F. Drake, V. Krasnoselskikh, S. Lejosne, and I. Vasko (2015), Time domain structures: What and where they are, what they do, and how they are made, *Geophys. Res. Lett.*, *42*, 3627–3638, doi:10.1002/2015GL063946.

Omura, Y., Y. Miyashita, M. Yoshikawa, D. Summers, M. Hikishima, Y. Ebihara, and Y. Kubota (2015), Formation process of relativistic electron flux through interaction with chorus emissions in the Earth's inner magnetosphere, *J. Geophys. Res. Space Physics*, *120*, 9545–9562, doi:10.1002/2015JA021563.

Sagdeev, R. Z. (1966), in *Reviews of Plasma Physics*, vol. 4, edited by M. A. Leontovich, p. 23, Consultants Bureau, New York.

Schulz, M., and L. J. Lanzerotti (1974), *Particle Diffusion in the Radiation Belts*, Springer, New York.

Shklyar, D., and H. Matsumoto (2009), Oblique whistler-mode waves in the inhomogeneous magnetospheric plasma: Resonant interactions with energetic charged particles, *Surv. Geophys.*, *30*, 55–104, doi:10.1007/s10712-009-9061-7.

Vasko, I. Y., O. V. Agapitov, F. S. Mozer, and A. V. Artemyev (2015a), Thermal electron interaction with electric field spikes in the outer radiation belt: Acceleration and formation of field-aligned pitch angle distributions, *J. Geophys. Res. Space Physics*, *120*, 8616–8632, doi:10.1002/2015JA021644.

Vasko, I. Y., O. V. Agapitov, F. S. Mozer, A. V. Artemyev, and D. Jovanovic (2015b), Magnetic field depression within electron holes, *Geophys. Res. Lett.*, *42*, 2123–2129, doi:10.1002/2015GL063370.

Watanabe, K., and T. Taniuti (1977), Electron-acoustic mode in a plasma of two-temperature electrons, *J. Phys. Soc. Jpn.*, *43*, 1819–1820.